Jaime J. L. Quispe, Tarcisio F. Maciel, Yuri C. B. Silva, and Anja Klein, "RIS-assisted beamforming for energy efficiency in multiuser downlink transmissions," in *Proc. IEEE Global Communications Conference Workshops (Globecom Workshops): Workshop on Emerging Topics in 6G Communications*, Rio de Janeiro, Brazil, December 2022.

©2022 IEEE. Personal use of this material is permitted. However, permission to reprint/republish this material for advertising or promotional purposes or for creating new collective works for resale or redistribution to servers or lists, or to reuse any copyrighted component of this works must be obtained from the IEEE.

RIS-assisted beamforming for energy efficiency in multiuser downlink transmissions

Jaime J. L. Quispe*, Tarcisio F. Maciel◇, Yuri C. B. Silva◇ and Anja Klein*
*Communications Engineering Lab, Technische Universität Darmstadt, Germany. Email:{j.luque, a.klein}@nt.tu-darmstadt.de
◇Wireless Telecom Research Group (GTEL), Federal University of Ceará, Brazil. Email:{maciel, yuri}@gtel.ufc.br

***Abstract*—Reconfigurable intelligent surface (RIS) based reflections is a promising approach to increase spectral efficiency (SE) and reduce power consumption of wireless communications systems. This paper investigates the trade-off between these two metrics by considering the energy efficiency (EE) maximization of an RIS-assisted multiuser downlink transmission from a multiantenna base station (BS) to multiple single-antenna users while satisfying constraints on quality-of-service (QoS), RIS phase shifts, and BS maximum transmit power. We consider a coordinated beamforming scheme and propose a joint optimization procedure based on the Dinkelbach, fractional programming, and semi-definite relaxation (SDR) methods. Simulation results show that the RIS-assisted system is more energy-efficient than its counterpart without RIS and that the RIS, particularly when it is equipped with a large number of antenna elements, can simultaneously improve the SE and power consumption of the transmission. Furthermore, the presented algorithm achieves good-quality solutions that are competitive to the obtained via exhaustive search with branch-reduce-and-bound (BRnB) methods and requires fewer iterations to converge.**

***Index Terms*—Reconfigurable intelligent surfaces, radio access networks, energy efficiency, multiuser transmissions, beamforming, sequential fractional programming, semi-definite relaxation.**

I. Introduction

The current deployment of radio access networks (RANs) raises concerns about the energy costs to operate the high-capacity base stations (BSs) [1]–[3]. Although the fifth-generation (5G) of mobile communications has more energy-saving features than its predecessors such as reduced always-on signaling, massive multiple-input multiple-output (MIMO) beamforming, and BS sleeping techniques [4], the high amount of energy required to compensate the path-loss of unfavorable propagation environments and to perform the MIMO operations still leaves room for improvement. In this regard, reconfigurable intelligent surface (RIS) is a promising nearly-passive antenna technology to enhance the wireless communication channel via passive beamforming [5]–[9]. Since it reflects the incoming radio-frequency (RF) waves in the desired directions without requiring power-hungry components, it can enable non-line-of-sight access and might help to alleviate such energy concerns. The received signals combine coherently, which increases the signal strength and the signal-to-noise (SNR) ratio. For example, studies [10], [11] have demonstrated that an N-element RIS increases the average SNR and reduces the amount-of-fading (AF) by a factor of N^2 and N, respectively. In [12], it was shown that by increasing N, it is possible to reduce the number of antennas at the BS without deteriorating the achievable rate at the user equipment (UE). That means fewer RF chains and fewer power amplifiers (PAs) at the BS. In addition, the effect of channel correlations on the SNR was analyzed in [13]. Other papers have shown the RIS benefits also in multiuser settings in terms of transmit power [10], signal-to-interference-plus-noise ratio (SINR) [14], and spectral efficiency (SE) [15]. While these papers studied the RIS contributions to either the SE or the power consumption, from the point of view of sustainability, it is worth noting that increasing the SE demands more power. The trade-off between these two metrics, i.e., the energy efficiency (EE), becomes then in a useful performance criterion that can guide system design. Unfortunately, we note there are very few studies that address this issue in the context of RIS.

The paper in [16] studies the EE of uplink multiuser MIMO in which approximate solutions for the UE transmit covariance matrices and RIS phase shifts are obtained jointly via fractional programming (FP) and majorization-minimization steps and it is shown that a RIS with 1-bit resolution phase shifts provides an EE gain of a factor of 2 w.r.t. the continuous case. For the downlink, [17] obtains the transmit powers and phase shifts via FP and gradient descent steps and reports an EE gain of a factor of 3 w.r.t. an amplify-and-forward relay. The application of RISs in cloud-RAN, which raises the EE concerns even further, is studied in [18], [19]. The first focuses on the EE fairness of a multicarrier uplink transmission and reports an increase of 20% on the worst EE w.r.t. a setup without RIS, whereas the second studies the downlink case and reports an increase of 30% via BS sleep decisions, link activations, and RIS reflections. Moreover, since it has been shown that centralized-coordinated systems can have better interference control than local processing approaches, the present paper adopts this scheme where the BS and RIS beamformers are jointly computed.

A. Scope and contributions

This paper investigates the EE maximization of an RIS-assisted multiuser downlink transmission and proposes a new

This work has been supported by the LOEWE Center emergenCITY, the BMBF project Open6GHub (grant no. 16KISK014), and the German Research Foundation (DFG) Collaborative Research Center (CRC) 1053 - MAKI (Nr. 210487104, projects B3, C1 and T2) and by DAAD with funds from the German Federal Ministry of Education and Research (BMBF). T. F. Maciel and Y. C. B. Silva also acknowledge the support of CNPq and CAPES/PROBRAL Grant 88887.144009/2017-00.

algorithm to jointly optimize the BS and RIS beamformers. Unlike [17], which assumes zero-forcing beamforming at the BS, our algorithm optimizes them for the best EE trade-off. Besides the reflected links, we consider the direct BS-UE links, and also minimum quality-of-service (QoS) requirements, which however were omitted in [16]. We consider the system is subject to a maximum BS transmit power and RIS phase-shift constraints. Unlike the exponential-complexity branch-reduce-and-bound (BRnB)-based algorithm in [19], our solution shows faster convergence, which allows comprehensive evaluation of the system performance. The associated EE problem is verified to be non-convex and is solved as an iterative algorithm that alternates the optimization of the beamformers using Dinkelbach [20], fractional programming [21] and semidefinite relaxation (SDR) [22] steps.

B. Paper outline and notation

The remainder of this paper is organized as follows. Section II presents the model of the RIS-assisted system as well as the EE problem formulation. Section III presents the proposed beamforming algorithm. Section IV presents the simulation setup and performance results, and Section V concludes this paper.

Notation: vectors, matrices, and sets are denoted as boldface lower case, boldface upper case and calligraphic letters, respectively. $\Re\{\cdot\}, \Im\{\cdot\}, (\cdot)^{\mathrm{T}}, |\cdot|, \|\cdot\|, \mathrm{diag}(\cdot), \mathrm{tr}(\cdot)$, denote the real part, imaginary part, transpose, modulus, Euclidean norm, diagonal, and trace operators. $(\cdot)^{\dagger}$ denotes either the complex conjugate transpose or complex conjugate operator, for vector and scalar argument, respectively. For any vector $\boldsymbol{x}$, x_m represents its m-th element, and $\boldsymbol{A} \succeq 0$ denotes that $\boldsymbol{A}$ is positive semidefinite.

II. System Model and Problem Formulation

A. RIS-assisted communication system

We consider a multiuser downlink system consisting of one N-antenna BS and K single-antenna UEs, as illustrated in Fig. 1. One RIS with M antenna-elements is installed to assist the communications. Each element $m \in \mathcal{M} \triangleq \{1, ..., M\}$ has a continuously tunable phase shifter of unit-amplitude, which can introduce a phase shift ϕ_m to the incident wave to change its direction. Let θ_m be the respective phase change and $\phi_m \triangleq e^{j\theta_m}$. The UEs are served in the same time-frequency resources using space division multiple access (SDMA) and we consider frequency-flat channels. The channel between the BS and the RIS is denoted by $\boldsymbol{H} \in \mathbb{C}^{M\times N}$, and, for each UE $k \in \mathcal{K} \triangleq \{1, ..., K\}$, the channels to the BS and to the RIS are denoted by $\boldsymbol{d}_k \in \mathbb{C}^{1\times N}$ and $\boldsymbol{g}_k \in \mathbb{C}^{1\times M}$, respectively. The BS and the RIS connect to a central processing unit (CPU). From knowledge of the channel responses, system requirements, and available resources, the CPU designs the best energy-efficient beamforming configurations and forward them to BS and RIS. The composite channel between the BS and UE k can be expressed as $\boldsymbol{h}_k(\boldsymbol{\phi}) \triangleq \boldsymbol{d}_k + \boldsymbol{g}_k \mathrm{diag}(\boldsymbol{\phi})\boldsymbol{H} \in \mathbb{C}^{1\times N}$, where $\boldsymbol{\phi} \triangleq [e^{j\theta_1}, ..., e^{j\theta_M}]^{\mathrm{T}}$. For every UE k, $s_k \sim \mathcal{CN}(0, 1)$

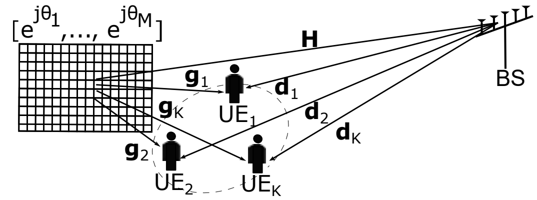

Fig. 1: RIS-assisted multiuser wireless communication system

represents the data symbol, $\boldsymbol{w}_k \in \mathbb{C}^{N\times 1}$ is the beamforming vector, and $n_k \sim \mathcal{CN}(0, \sigma^2)$ is the receiver noise of variance σ^2. The received signal can be modeled as $y_k = \boldsymbol{h}_k \boldsymbol{w}_k s_k + \sum_{j\in\mathcal{K}\setminus\{k\}} \boldsymbol{h}_k \boldsymbol{w}_j s_j + n_k$, and if $\mathcal{W} \triangleq \{\boldsymbol{w}_k\}_{k\in\mathcal{K}}$, the SE of UE k can be expressed as

$$r_k(\mathcal{W}, \boldsymbol{\phi}) = \log_2\left(1 + \frac{|\boldsymbol{h}_k \boldsymbol{w}_k|^2}{\sum\limits_{j\in\mathcal{K}\setminus\{k\}} |\boldsymbol{h}_k \boldsymbol{w}_j|^2 + \sigma^2}\right) \text{bit/s/Hz}, \tag{1}$$

where the ratio term inside the log function is the SINR at UE k. We consider that each UE k has a minimum QoS requirement $r_{\min,k}$, i.e.,

$$r_k(\mathcal{W}, \boldsymbol{\phi}) \geq r_{\min,k}. \tag{2}$$

The power consumption of the considered system is composed of the RIS circuit power dissipation, which is denoted by P_o, and the transmit power. Each RIS element has a power consumption P_e, i.e., $P_o = MP_e$. Moreover, the PAs operate in its linear region with constant efficiency denoted by η_o. Therefore, the power consumption can be modeled as

$$p(\mathcal{W}) = \tfrac{1}{\eta_o} \sum\nolimits_{k\in\mathcal{K}} \|\boldsymbol{w}_k\|^2 + P_o. \tag{3}$$

We assume the BS has limited power resources and has a maximum transmit power budget of $P_{\max}$, i.e.,

$$\sum\nolimits_{k\in\mathcal{K}} \|\boldsymbol{w}_k\|^2 \leq P_{\max}. \tag{4}$$

B. Problem formulation

For the proposed system, the maximum EE and joint BS-RIS beamforming problem can be formulated as

$$\mathcal{P}_1 : \eta^* = \max_{\boldsymbol{\phi}, \mathcal{W}} \frac{\sum_{k\in\mathcal{K}} r_k(\mathcal{W}, \boldsymbol{\phi})}{p(\mathcal{W})}, \tag{5}$$

$$\text{s.t.: } (2), (4),$$

$$|\phi_m| = 1, \forall m \in \mathcal{M}, \tag{6}$$

where the RIS unit-amplitude constraint is given by (6). Observe that both the BS and RIS beamforming vectors are coupled together in the SINR terms in (2) and (5), and (6) is a non convex constraint. Moreover, the fractional objective function does not have a concave-convex form and its numerator is composed of the sum of ratio terms. For these reasons, it is difficult to optimally solve $\mathcal{P}_1$. Therefore, the aim of this paper is a stationary feasible solution of low complexity. Particularly, the concavity of the logarithm function and the convexity of the denominator are exploited to express (5) in auxiliary concave functions suitable for alternating optimization. In section III, we tackle the aforementioned difficulties by employing Dinkelbach and quadratic FP transformations. We apply a SDR to the RIS-related constraints plus an eigenvector-based phase-shift recovery. The procedure is presented in an iterative algorithm that alternates the optimization of the BS and RIS beamformers.

III. RIS-ASSISTED BEAMFORMING FOR ENERGY EFFICIENCY

In this section, we propose an alternating algorithm to find a stationary feasible solution of $\mathcal{P}_1$.

A. BS beamforming optimization

Since $r_k(\mathcal{W},\boldsymbol{\phi}) \geq 0$ and $p(\mathcal{W}) > 0$, and both (2) and (4) represent closed and bounded subsets, we can introduce an auxiliary parameter α to express the objective function of (5) as a difference of functions and reformulate $\mathcal{P}_1$ via the Dinkelbach transformation [20] as

$$\mathcal{P}_2 : \max_{\boldsymbol{\phi},\mathcal{W},\alpha} \sum_{k\in\mathcal{K}} r_k\left(\mathcal{W},\boldsymbol{\phi}\right) - \alpha p(\mathcal{W}), \tag{7}$$
$$\text{s.t.: } (2),(4),(6).$$

However, since the original objective does not have a concave-convex fractional form and the search set for $\boldsymbol{\phi}$ is non-convex, $\mathcal{P}_2$ remains non-convex for given α. In this case we use an approximate solution of $\mathcal{P}_2$ for the update of α in the next iteration. If we fix $\boldsymbol{\phi}$, (7) remains non-concave and we cannot decouple each k-th SINR inside the logarithm because the objective value in (7) is not preserved across successive iterations [21]. In this case, from the quadratic FP transformation method [21, Corollary 1], we can introduce an auxiliary variable z_k to express each SINR term into an auxiliary function

$$\vartheta_k(\mathcal{W},\boldsymbol{z}) = 2\Re\{z_k^\dagger \boldsymbol{h}_k\boldsymbol{w}_k\} - |z_k|^2\Big(\sum_{j\in\mathcal{K}\setminus\{k\}} |\boldsymbol{h}_k\boldsymbol{w}_j|^2 + \sigma^2\Big). \tag{8}$$

Therefore, $\mathcal{P}_2$ can be equivalently represented as

$$\mathcal{P}_3 : \max_{\mathcal{W}} \sum_{k\in\mathcal{K}} \log_2\left(1 + \max_{z_k} \vartheta_k(\mathcal{W},\boldsymbol{z})\right) - \alpha p(\mathcal{W}), \tag{9}$$
$$\text{s.t.: } (2),(4).$$

Note that for given $\mathcal{W}$, the optimal z_k^* in the inner maximization of (9) can be obtained via solving $\frac{\partial \vartheta_k}{\partial z_k} = 0$. Let n and $n-1$ be the current and previous iteration indexes, respectively. Then z_k^* can be updated as

$$z_k^* = \frac{\boldsymbol{h}_k\boldsymbol{w}_k^{n-1}}{\sum_{j\in\mathcal{K}\setminus\{k\}} |\boldsymbol{h}_k\boldsymbol{w}_j^{n-1}|^2 + \sigma^2}. \tag{10}$$

With the recast objective (9), α can be updated as [20]

$$\alpha^{(n)} = \frac{\sum_{k\in\mathcal{K}} \log_2\left(1 + \vartheta_k(\mathcal{W}^{(n-1)},\boldsymbol{z}^*)\right)}{\frac{1}{\eta_{\text{PA}}}\sum_{k\in\mathcal{K}} \|\boldsymbol{w}_k^{(n-1)}\|^2 + P_o}, \tag{11}$$

where the upper index $n-1$ refers to the results from the previous iteration. Then, $\mathcal{P}_3$ can be reformulated as

$$\mathcal{P}_4 : \max_{\mathcal{W}} \sum_{k\in\mathcal{K}} \log_2\left(1 + \vartheta_k(\mathcal{W},\boldsymbol{z}^*)\right) - \alpha p(\mathcal{W}), \tag{12}$$
$$\text{s.t.: } \boldsymbol{h}_k\boldsymbol{w}_k \geq \sqrt{\gamma_{\min,k} \sum_{j\in\mathcal{K}\setminus\{k\}} (|\boldsymbol{h}_k\boldsymbol{w}_j|^2 + \sigma^2)}, \forall k, \tag{13}$$
$$\Im(\boldsymbol{h}_k\boldsymbol{w}_k) = 0, \forall k, \tag{14}$$
$$\text{and } (4),$$

where $\gamma_{\min,k} \triangleq 2^{r_{\min,k}} - 1$ is the required minimum SINR for UE k and (13) and (14) are the second-order cone (SOC) and linear forms from (2). Observe that since each logarithm function is concave and increasing and its new quadratic argument $\vartheta_k(\mathcal{W}, z^*)$ is also concave, $\mathcal{P}_4$ is a convex problem and can be solved, for instance, using CVX and Mosek [23].

B. RIS beamforming optimization

With $\mathcal{W}$ fixed, by introducing K auxiliary variables $t_k, k = 1, ..., K$, each SINR term in (7) can be rewritten as

$$\psi_k(\boldsymbol{\phi},\boldsymbol{t}) = 2\Re\{t_k^\dagger \boldsymbol{h}_k(\boldsymbol{\phi})\boldsymbol{w}_k\} - |t_k|^2\left(\sum_{j\in\mathcal{K}\setminus\{k\}} |\boldsymbol{h}_k(\boldsymbol{\phi})\boldsymbol{w}_j|^2 + \sigma^2\right). \tag{15}$$

Therefore, similar to the BS beamforming optimization in $\mathcal{P}_3$, $\mathcal{P}_2$ can be reformulated as

$$\mathcal{P}_5 : \max_{\boldsymbol{\phi}} \sum_{k\in\mathcal{K}} \log_2(1 + \max_{t_k} \psi_k(\boldsymbol{\phi},\boldsymbol{t})), \tag{16}$$
$$\text{s.t.: } (2),(6),$$

where t_k can be updated as

$$t_k = \frac{\boldsymbol{h}_k(\boldsymbol{\phi}^{(n-1)})\boldsymbol{w}_k^*}{\sum_{j\in\mathcal{K}\setminus\{k\}} |\boldsymbol{h}_k(\boldsymbol{\phi}^{(n-1)})\boldsymbol{w}_j^*|^2 + \sigma^2}, \tag{17}$$

with $\boldsymbol{\phi}^{(n-1)}$ and $\boldsymbol{w}^*$ denoting the RIS phase-shifts obtained in the previous iteration $n-1$ and the optimal solution of $\mathcal{P}_4$, respectively. If we fix $\boldsymbol{t}$ and define $c_{kj} \triangleq \boldsymbol{d}_k\boldsymbol{w}_j \in \mathbb{C}$, $\boldsymbol{e}_{kj} \triangleq \text{diag}(\boldsymbol{g}_k)\boldsymbol{H}\boldsymbol{w}_j \in \mathbb{C}^{M\times 1}$, $\mathcal{P}_5$ can be reformulated as

$$\mathcal{P}_6 : \max_{\boldsymbol{\phi}} \sum_{k\in\mathcal{K}} \log_2\left(1 + 2\Re\{\boldsymbol{\phi}^T\boldsymbol{a}_k\} - \boldsymbol{\phi}^T\boldsymbol{Q}_k\boldsymbol{\phi}^* + \xi_k\right) \tag{18}$$
$$\text{s.t.: } (2),(6),$$

where for each $k \in \mathcal{K}$, $\boldsymbol{a}_k$, $\boldsymbol{Q}_k$ and ξ_k are given by

$$\boldsymbol{a}_k = t_k^\dagger\boldsymbol{e}_{kk} - \sum_{j\in\mathcal{K}\setminus\{k\}} |t_k|^2 \boldsymbol{e}_{kj}c_{kj}^\dagger, \tag{19}$$

$$\boldsymbol{Q}_k = |t_k|^2 \sum_{j\in\mathcal{K}\setminus\{k\}} \boldsymbol{e}_{kj}\boldsymbol{e}_{kj}^\dagger, \text{ and} \tag{20}$$

$$\xi_k = 2\Re\{t_k^\dagger c_{kk}\} - |t_k|^2 \sum_{j\in\mathcal{K}\setminus\{k\}} |c_{kj}|^2 - |t_k|^2\sigma^2, \tag{21}$$

respectively, with $\boldsymbol{Q}_k$ being Hermitian. Then, by defining $\boldsymbol{\phi}^T \triangleq \boldsymbol{x}^\dagger$ and $\boldsymbol{R}_{kj} \triangleq \begin{bmatrix} \boldsymbol{e}_{kj}\boldsymbol{e}_{kj}^\dagger & \boldsymbol{e}_{kj}c_{kj}^* \\ c_{kj}\boldsymbol{e}_{kj}^\dagger & 0 \end{bmatrix} \in \mathbb{C}^{M+1\times M+1}$, and introducing a new variable $\boldsymbol{X} \triangleq [\begin{smallmatrix}\boldsymbol{x}\\1\end{smallmatrix}][\begin{smallmatrix}\boldsymbol{x}\\1\end{smallmatrix}]^\dagger$, $\mathcal{P}_6$ can be equivalently reformulated as

$$\mathcal{P}_7: \max_{\boldsymbol{x},\boldsymbol{X}\succeq 0} \sum_{k\in\mathcal{K}} \log_2\left(1 + 2\Re\{\boldsymbol{x}^\dagger \boldsymbol{a}_k\} - \boldsymbol{x}^\dagger \boldsymbol{Q}_k \boldsymbol{x} + \xi_k\right) \quad (22)$$

$$\text{s.t. }: \boldsymbol{X} = [\begin{smallmatrix}\boldsymbol{x}\\1\end{smallmatrix}][\begin{smallmatrix}\boldsymbol{x}\\1\end{smallmatrix}]^\dagger, \quad (23)$$

$$\boldsymbol{X}_{mm} = 1, \forall m \in \mathcal{M}, \quad (24)$$

$$\mathrm{tr}(\boldsymbol{R}_{kk}\boldsymbol{X}) + |c_{kk}|^2 \geq \gamma_{\min,k} \sum_{j\in\mathcal{K}\setminus\{k\}} \Big(\mathrm{tr}(\boldsymbol{R}_{kj}\boldsymbol{X}) + |c_{kj}|^2 + \sigma^2\Big), \forall k \in \mathcal{K}, \quad (25)$$

where for every $k \in \mathcal{K}$, (2) has been transformed to the SOC constraint (25). Observe that $\mathcal{P}_7$ is a unit-amplitude complex quadratically-constrained quadratic problem (CQCQP), which has been shown to be NP-hard [24], [25]. We apply the semidefinite relaxation developed in [25] and rewrite the constraint (23) as $\boldsymbol{X} \succeq [\begin{smallmatrix}\boldsymbol{x}\\1\end{smallmatrix}][\begin{smallmatrix}\boldsymbol{x}\\1\end{smallmatrix}]^\dagger$, which, together with (24), implies $\boldsymbol{x} \leq 1$, i.e., the obtained RIS phase shifts can have at most unit amplitudes. The modified constraint allows to solve $\mathcal{P}_7$ via semidefinite programming (SDP). Then, the best rank-one approximation [22] of the upper-bound solution $\boldsymbol{X}^*$ can be expressed as $\hat{\boldsymbol{X}} = \sqrt{\lambda}\boldsymbol{u}\boldsymbol{u}^T$, where λ is the largest eigenvalue of $\boldsymbol{X}^*$ and $\boldsymbol{u}$ is its corresponding eigenvector. Consequently, we can extract an approximate solution for each phase-shift via projection as $\phi_m = \frac{u_m^\dagger}{|u_m|}, \forall m \in \mathcal{M}$. The steps for solving $\mathcal{P}_1$ are summarized in Algorithm 1.

Algorithm 1: Iterative algorithm for solving $\mathcal{P}_1$.

Result: $\eta^*, \mathcal{W}^*, \boldsymbol{\phi}^*$
1: initialize $\mathcal{W}$ and $\boldsymbol{\phi}$, set precision ϵ, iteration $n = 1$
2: **while** $(\alpha^n - \alpha^{n-1})/\alpha^{n-1} > \epsilon$ **do**
3: compute optimal $\boldsymbol{z}^*$ using (10)
4: compute α using (11)
5: solve $\mathcal{P}_4$ of (12) – (14) and get $\mathcal{W}$
6: compute optimal $\boldsymbol{t}$ using (17)
7: solve $\mathcal{P}_7$ of (22) – (25) and get $\boldsymbol{X}^*$
8: extract $\boldsymbol{\phi}$ from the best eigenvector.
9: **end while**

IV. Numerical Results

We consider a picocell-based industrial setup composed of one four-antenna BS, a M-antenna RIS and three single-antenna UEs, i.e., $N = 4$ and $K = 3$. The RIS and BS antennas are located at coordinates (0, 0, 8)m and (200, 0, 10)m, respectively, i.e., the RIS and the BS are separated by a horizontal distance of d_{BR} =200m. The UEs are positioned randomly on a circle of radius 25m between the BS and the RIS and at a height of 1m, as illustrated in Fig. 1. The center of such circle is set at the xy coordinates (26, 0)m. For each UE$_k$, the distances RIS-UE$_k$ and BS-UE$_k$ are denoted as $d_{\text{RU},k}$ and $d_{\text{BU},k}$, respectively. We consider that the composite BS-RIS-UE$_k$ channel is double-fading with large-scale path-loss coefficient $\beta_{\text{BRU},k} = C_{\text{BRU}} d_{\text{BR}}^{-\kappa_1} d_{\text{RU},k}^{-\kappa_2}$, and that the BS-UE$_k$ path-loss is $\beta_{\text{BU},k} = C_{\text{BU}} d_{\text{BU},k}^{-\kappa_3}$, where $C_{\text{BRU}} = -30$dB,

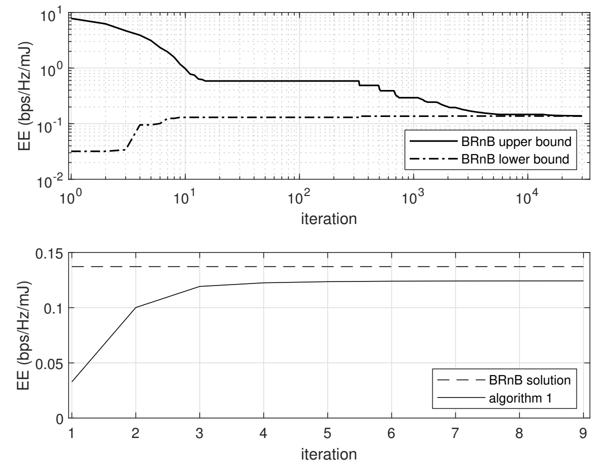

Fig. 2: Convergence of the proposed algorithm and comparison with the BRnB benchmark. $N = 4$, $M = 4$, $K = 3$, $P_o =$ 5dBm, $P_{\max} = 27$dBm, $r_{\min,k} = 0$.

$C_{\text{BU}} = -30$dB, $\kappa_1 = 2$, $\kappa_2 = 2$, and $\kappa_3 = 3.5$, as studied in [10], [26]. Also, we consider small-scale Rayleigh fading for the three sets of channels $\boldsymbol{H}$, $\{\boldsymbol{g}_k\}_\mathcal{K}$ and $\{\boldsymbol{d}_k\}_\mathcal{K}$. We set $\sigma^2 = -96$dBm, $P_{\max} = 33$dBm, $P_e = 10$dBm [17], [27], $\eta_o = 0.3$. We consider the following benchmarks: 1) the BRnB-based EE maximization method [19], which obtains the BS and RIS beamformers and link activation decisions via monotonic optimization; 2) baseline: the system without RIS optimized for EE with a variant of our proposed algorithm which bypass the RIS beamforming steps, i.e., lines 6, 7 and 8 of Alg. 1; 3) fixed: the system with a RIS unable to reconfigure its elements where the phase-shifts are initialized randomly and kept fixed along the iterations; 4) SRMax: the system configured for maximum rate using also a variant of Alg. 1 where the optimization is performed only over the numerator of (5). The convergence of such algorithm is established by the convergence of the objective function in (22).

We set $r_{\min,k} = 0$ bits/s/Hz $\forall k$ in order to let the algorithm find the best rate-power tradeoff, and include a QoS case with $r_{\min,k} = 8, \forall k$. The algorithm precision $\epsilon = 10^{-3}$, system parameters, and UE positions are the same for the proposed method and for the benchmarks.

Fig. 2 presents the algorithm convergence for one channel realization, with $M = 4$. The phase-shifts are all initialized at 90^o and each $\boldsymbol{w}_k$ as a conjugated beamformer matched to the respective direct channel $\boldsymbol{h}_k$ with power $P_{\max}/K$. We observe that Alg. 1 requires only a small number of iterations for convergence and obtains a solution with an EE of approximately 90% of the reference BRnB algorithm. Therefore, it can be considered as a more efficient way to evaluate the EE of RIS-assisted communication systems.

Fig. 3 compares the cumulative density function (CDF) of the achieved EE over 2000 channel realizations when $M = 16$ and $M = 32$. For both RIS sizes, the system optimized with Alg. 1 provides higher EE than the baseline. At the 90% likely EE points, such gains are approximately a factor of 9

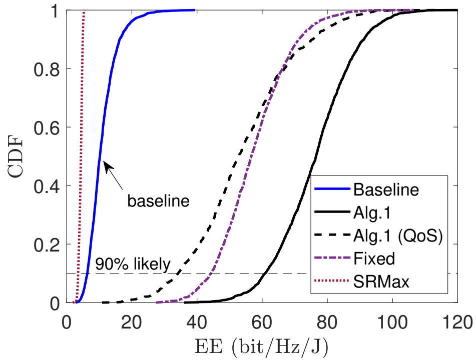

(a) $M = 16$

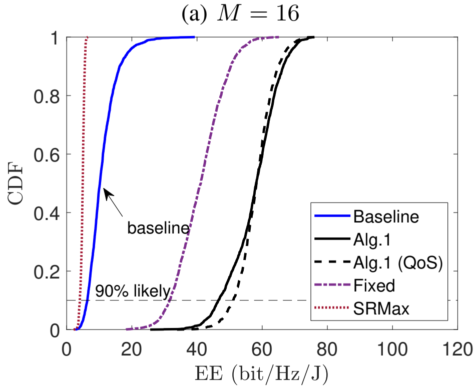

(b) $M = 32$

Fig. 3: Comparison of the system EE with two RIS sizes and different algorithm benchmarks.

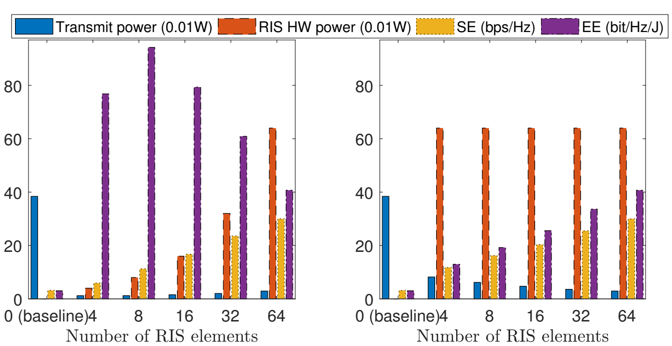

Fig. 4: Power consumption, SE, and EE of the RIS system.

and 7, respectively, and, in the QoS case, a factor of 5 and 8, respectively. This is because, with more antenna elements, there are more channel paths, which the RIS manipulates to increase the beamforming gains. It can be seen that the impact of the QoS requirement on the achievable EE is higher when the RIS is smaller. This is because a higher QoS requires higher transmit power. On the other hand, the larger RIS enables higher UE rates and power savings. It can also be seen the performance loss in the cases Fixed and SRMax. For the latter, the loss is approximately a factor of 11 w.r.t. Alg. 1 when $M = 32$ because the BS transmits with power $P_{\max}$. Fig. 4, presents the average power consumption, sum-rate and EE achieved with Alg. 1 for two cases of RIS hardware power

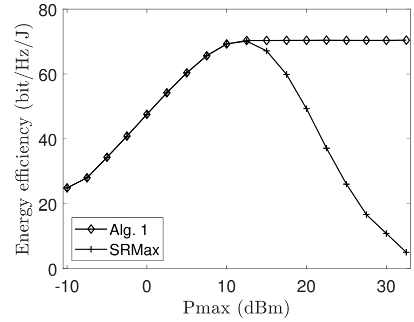

Fig. 5: EE performance for different transmit power budgets

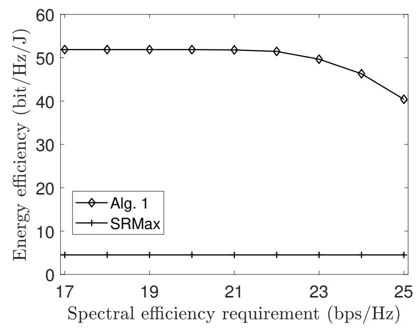

Fig. 6: EE performance for different SE requirements

consumption P_o: when it scales with RIS size, i.e., $P_o = MP_e$ (left) or when it is constant (right). In the first case, the EE increases until a certain threshold on the number of elements after which P_o dominates the total power consumption. In the second case, it can be observed that both the SE and the power consumption improve when the RIS is equipped with more antenna elements. In both cases the SE also increases with the RIS size and the system achieves better EE than the baseline system, which is in agreement with the results in Fig. 3.

Fig. 5 compares the EE performance of Alg. 1 and SRMax for different transmit power budgets. We observe that the EE increases with $P_{\max}$ until a certain threshold, which corresponds to the transmit power for maximum EE. An excess on this power causes a rapid degradation of the performance when the system is optimized via SRMax. On the other hand, Alg. 1 avoids using more power than necessary to preserve the optimal state.

In order to study the QoS case, we introduce a minimum sum SE requirement, which is denoted by ρ, by adding the constraint $\sum_{k\in\mathcal{K}} \log_2\left(1 + \vartheta_k(\mathcal{W}, \boldsymbol{z}^*)\right) \geq \rho$ to $\mathcal{P}_4$ and the corresponding feasibility verification to $\mathcal{P}_7$. We set $r_{\min,k} = 0, \forall k$. Fig. 6 shows the EE performance for different values of ρ. We observe that the system has also a SE threshold at which it achieves its maximum performance. The EE is significantly reduced above this threshold because the power consumption increases with the SE requirement. Alg. 1 maintains the EE performance for increasing values of ρ below the threshold.

Fig. 7 shows the EE for different UE positions. The value of P_o is set very low in order to analyze the trade-off between SE and transmit power. The center of the cluster of UEs is

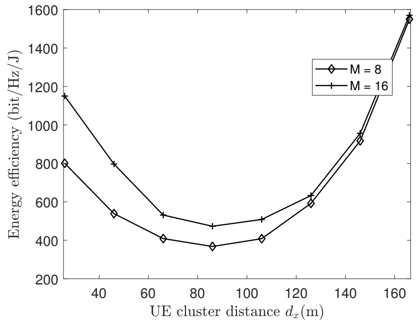

Fig. 7: EE performance for different UE positions

set at the xy coordinates (d_x, 0)m. The positions d_x =26m and d_x =166m represent the scenarios when UEs are closer to the RIS or to the BS, respectively. It can be observed that the contribution of the RIS is higher when the UEs are closer to it, i.e., the RIS extends the range of coverage and alleviates the transmit power consumption. The contribution decreases as the UEs get closer to the BS, where higher EE is possible due to the reduced path-loss of the direct BS-UEs channels.

V. Conclusion

In this paper, we considered an RIS-assisted multiuser downlink system and presented a procedure for joint optimization of the BS and RIS beamformers for maximum energy efficiency. The alternating algorithm was based on the Dinkelbach, fractional programming, and semidefinite relaxation methods. Numerical simulations showed that the algorithm is able to provide a solution with 90% of the achievable EE obtained via exhaustive-search with BRnB methods while requiring fewer iterations to converge. Benchmark algorithms for maximizing the SE of the RIS-assisted system and the EE of a baseline system without a RIS were presented as special cases. With an RIS equipped with 32 antenna-elements optimized for EE, the system is 11 and 7 times more energy efficient than the mentioned benchmarks. It was observed that higher QoS requirements can be met without deteriorating the EE using a larger RIS and that both the SE and power consumption can be simultaneously improved. Furthermore, it was seen that EE grows with the available transmit power budget until a certain threshold, which is optimized by the proposed method. Moreover, it was seen that the RIS can extend the coverage, and the closer it is to the UEs, the higher its contribution to the EE.

References

[1] S. Han, T. Xie and C-L. I, "Greener Physical Layer Technologies for 6G Mobile Communications," *IEEE Commun. Mag.*, Vol. 59, No. 4, pp. 68-74, 2021.

[2] S. Zhang, Q. Wu, S. Xu and G. Y. Li, "Fundamental Green Tradeoffs: Progresses, Challenges, and Impacts on 5G Networks," *IEEE Commun. Surveys & Tutorials*, Vol. 19, No. 1, pp. 33-56, 2017.

[3] B. Zahnstecher, "The 5G Energy Gap [Expert View]," *IEEE Power Electron. Mag.*, Vol. 6, No. 4, pp. 64-67, 2019.

[4] E. Dahlman, S. Parkvall, and J. Sköld, *5G NR: The Next Generation Wireless Access Technology*, 2nd ed., Academic Press, 2020.

[5] Y. Liu et al., "Reconfigurable Intelligent Surfaces: Principles and Opportunities," *IEEE Commun. Surveys & Tutorials*, Vol. 23, No. 3, pp. 1546-1577, 2021.

[6] Q. Wu, S. Zhang, B. Zheng, C. You and R. Zhang, "Intelligent Reflecting Surface-Aided Wireless Communications: A Tutorial," *IEEE Trans. on Commun.*, Vol. 69, No. 5, pp. 3313-3351, 2021.

[7] R. Liu, Q. Wu, M. Di Renzo and Y. Yuan, "A Path to Smart Radio Environments: An Industrial Viewpoint on Reconfigurable Intelligent Surfaces," *IEEE Wireless Commun.*, Vol. 29, No. 1, pp. 202-208, 2022.

[8] G. C. Trichopoulos et al., "Design and Evaluation of Reconfigurable Intelligent Surfaces in Real-World Environment," *IEEE Open J. of the Commun. Soc.*, Vol. 3, pp. 462-474, 2022.

[9] X. Pei et al., "RIS-Aided Wireless Communications: Prototyping, Adaptive Beamforming, and Indoor/Outdoor Field Trials," *IEEE Trans. on Commun.*, Vol. 69, No. 12, pp. 8627-8640, 2021.

[10] Q. Wu and R. Zhang, "Intelligent Reflecting Surface Enhanced Wireless Network via Joint Active and Passive Beamforming," *IEEE Trans. Wireless Commun.*, Vol. 18, No. 11, pp. 5394-5409, 2019.

[11] X. Qian, M. Di Renzo, J. Liu, A. Kammoun and M.S. Alouini, "Beamforming Through Reconfigurable Intelligent Surfaces in Single-User MIMO Systems: SNR Distribution and Scaling Laws in the Presence of Channel Fading and Phase Noise," *IEEE Wireless Commun. Letters*, Vol. 10, No. 1, pp. 77-81, 2021.

[12] X. Yu, D. Xu and R. Schober, "Optimal Beamforming for MISO Communications via Intelligent Reflecting Surfaces," *IEEE Int. Workshop on Signal Process. Advances in Wireless Commun.*, pp. 1-5, 2020.

[13] A. Almohamad, M. Hasna, N. Zorba and T. Khattab, "Performance of THz Communications Over Cascaded RISs: A Practical Solution to the Over-Determined Formulation," *IEEE Commun. Letters*, Vol. 26, No. 2, pp. 291-295, 2022.

[14] Q-U-A. Nadeem, A. Kammoun, A. Chaaban, M. Debbah and M.S. Alouini, "Asymptotic Max-Min SINR Analysis of Reconfigurable Intelligent Surface Assisted MISO Systems," *IEEE Trans. Wireless Commun.*, Vol. 19, No. 12, pp. 7748-7764, 2020.

[15] H. Guo, Y. Liang, J. Chen and E. G. Larsson, "Weighted Sum-Rate Maximization for Reconfigurable Intelligent Surface Aided Wireless Networks," *IEEE Trans. on Wireless Commun.*, Vol. 19, No. 5, pp. 3064-3076, 2020.

[16] J. Xiong, L. You, D. W. K. Ng, C. Yuen, W. Wang and X. Gao, "Energy Efficiency and Spectral Efficiency Tradeoff in RIS-Aided Multiuser MIMO Uplink Systems," *IEEE Global Commun. Conf.*, 2020.

[17] C. Huang, A. Zappone, G. C. Alexandropoulos, M. Debbah and C. Yuen, "Reconfigurable Intelligent Surfaces for Energy Efficiency in Wireless Communication," *IEEE Trans. Wireless Commun.*, vol. 18, no. 8, pp. 4157-4170, 2019.

[18] K. Liu and Z. Zhang, "On The Energy-Efficiency Fairness of Reconfigurable Intelligent Surface-Aided Cell-Free Network," *IEEE Veh. Technol. Conf. (VTC2021-Spring)*, 2021, pp. 1-6.

[19] J. J. L. Quispe, T. F. Maciel, Y. C. B. Silva and A. Klein, "Beamforming and link activation methods for energy efficient RIS-aided transmissions in C-RANs," *IEEE Global Commun. Conf.*, pp. 1-6, 2021.

[20] W. Dinkelbach, "On nonlinear fractional programming," *Manage. Sci.*, vol. 133, no. 7, pp. 492–498, 1967.

[21] S. Kaiming and Y. Wei, "Fractional Programming for Communication Systems—Part I: Power Control and Beamforming," *IEEE Trans. on Signal Process.*, vol. 66, no. 10, pp. 2616-2630, 2018.

[22] Z. Luo, W. Ma, A. So, Y. Ye and S. Zhang, "Semidefinite Relaxation of Quadratic Optimization Problems," *IEEE Signal Process. Mag.*, Vol. 27, No. 3, pp. 20-34. 2010.

[23] CVX Research, Inc., "CVX: Matlab Software for Disciplined Convex Programming, version 2.0," 2012, *http://cvxr.com/cvx*.

[24] S. Zhang and Y. Huang, "Complex Quadratic Optimization and Semidefinite Programming," *SIAM J. on Optim.*, vol. 16, no. 3, pp. 871-890, 2006.

[25] L. Cheng, D. Zhibin, W. Zhang and S. Fang, "Argument division based branch-and-bound algorithm for unit-modulus constrained complex quadratic programming," *J. Glob. Optim.*, vol. 70, no. 1, pp. 171-187, 2018.

[26] Z. Zhang and L. Dai, "A Joint Precoding Framework for Wideband Reconfigurable Intelligent Surface-Aided Cell-Free Network," *IEEE Trans. Signal Process.*, vol. 69, pp. 4085-4101, 2021.

[27] Y. Zhang et al., "Beyond Cell-Free MIMO: Energy Efficient Reconfigurable Intelligent Surface Aided Cell-Free MIMO Communications," *IEEE Trans. Cogn. Commun. Netw.*, Vol. 7, No. 2, pp. 412-426, 2021.